A point-by-point response to Referee #1

We sincerely appreciate Referee #1 for the valuable comments and constructive suggestions that helped improve the quality of our manuscript. The following is a point-by-point response to address the referee's comments. The original comments are shown in *black*, and our corresponding responses are presented in *blue*. The new or modified contents in the revised manuscript are marked in *red*.

Comments from Referee #1:

This manuscript studied HONO concentrations and its sources in urban Beijing during autumn and winter of 2022. The results showed that NO_2 heterogeneous reaction on ground was the dominant HONO source. Vehicle emissions and nitrate photolysis also contributed to HONO concentrations. In general, the research is interesting, the results and discussions are sounds. Here are some technique comments need to be addressed before it can be accepted.

Response: Many thanks to Referee #1 for the valuable comments and constructive suggestions, which are significant for improving the quality of the manuscript. We carefully revised and supplemented the manuscript in response to the referee's comments on the technique comments. The following are point-by-point responses to the referee's comments.

Detailed comments:

1. L78, studied.

Response: Thanks for your valuable comments. Revision has been made as the referee suggested. Lines 80-82 in the revised manuscript:

"It provided a unique opportunity to identify HONO sources and their potential impact to secondary pollution formation in urban Beijing, which has been rarely studied in the past."

2. L114-115, the NO concentrations measured by chemiluminescence NOx analyzer is ok. But the analyzer could overestimate NO_2 concentrations due to include other oxidized nitrogen. You can calibrate the data using the method in JGR: Atmospheres, 127, e2021JD036379. https://doi.org/10.1029/2021JD036379.

Response: Thanks for your valuable comments. Revision was made as the referee suggested. We corrected CL_NO_2 (Thermo Scientific, Model 42i NOx analyzer) using interference-free CAPS_NO_2 measurements (Teledyne API-N500 NOx analyzer), and provided rigorous field comparison evidence. To improve the precision and accuracy of the NO_2 correction, we established separate daytime and nighttime linear regressions. All relevant parameters were recalculated with the corrected NO_2, and the model simulations were rerun. The correction methodology and its impacts were described in detail in the Supporting Information (see Text S1 and Figure S1).

Text S1 in the Supporting Information:

"As the most important precursor of HONO, accurate measurement of NO_2 was crucial for analyzing HONO formation. A commercial Thermo Scientific analyzer (42i) used in this study could specifically detect NO. The measurement of NO_2 was achieved by converting NO_2 to NO through a molybdenum converter. However, the chemiluminescence (CL) technique could overestimate NO_2 concentrations because of the interference of NOy. These interferences included HONO, HNO_3, HNO_4, N_2O_5, NO_3, peroxyacetyl nitrate (PANs, $RC(O)OONO_2$), organic nitrates ($RONO_2$), and peroxynitrates ($ROONO_2$) (Villena et al., 2012; Wu et al., 2022). Therefore, the NO_2 measured by the CL-NOx analyzer represented the sum of real NO_2 and these interfering species. In contrast, the commercial Teledyne API-N500 NOx analyzer was based on cavity attenuated phase shift (CAPS) technique. It could provide direct absorption measurement of NO_2 at 450 nm in the blue region of the electromagnetic spectrum, allowed fast and accurate detection of NO_2 without interference from water vapor. The only known potential interferences in the typical ambient environment were dicarbonyl compounds such as glyoxal and methylglyoxal, whose concentrations were usually much lower than NO_2 mixing ratios (Kebabian et al., 2008). Therefore, NO_2 measured by the CAPS-NOx analyzer (CAPS_NO_2) could be used to correct the NO_2 measured by the CL-NOx analyzer (CL_NO_2).

We conducted a NO_2 field campaign at the ICCAS site from September 19 to October 11, 2023, to compare the performance of the CL-NOx and CAPS-NOx analyzers. The sampling inlets of both instruments were placed at the same location, with identical sampling tube lengths, and the analyzers were housed in the same indoor environment to minimize external interference. The results showed that CAPS_NO_2 and CL_NO_2 exhibited similar temporal variations (Figure S1(a) and S1(b)). Notably, CL_NO_2 was consistently higher than CAPS_NO_2, with a more pronounced difference during the daytime. This discrepancy was mainly attributed to elevated NOy concentrations caused by enhanced photochemical reactions. Consequently, the fraction of CAPS_NO_2 in CL_NO_2 displayed a distinct diurnal pattern, being higher at night and lower during the day (Figure S1(c)), which was consistent with previous findings (Xue et al., 2022; Zhang et al., 2022c). Based on this result, we applied separate calibrations for daytime (07:00-18:00 LT) and nighttime (19:00-next 06:00 LT) data. The results indicated strong linear correlations between CAPS_NO_2 and CL_NO_2 during both periods ($R^2 = 0.96$ for daytime and $R^2 = 0.95$ for nighttime). The regression equations were "$y = 0.98x - 2.27$" for daytime and "$y = 0.99x - 2.29$" for nighttime, where y represented CAPS_NO_2 and x represented CL_NO_2 (Figure S1(d) and S1(e)). Using these relationships to correct the NO_2 data obtained in this study provided a more reasonable estimation of true NO_2 concentrations and offered a reliable basis for further analysis."

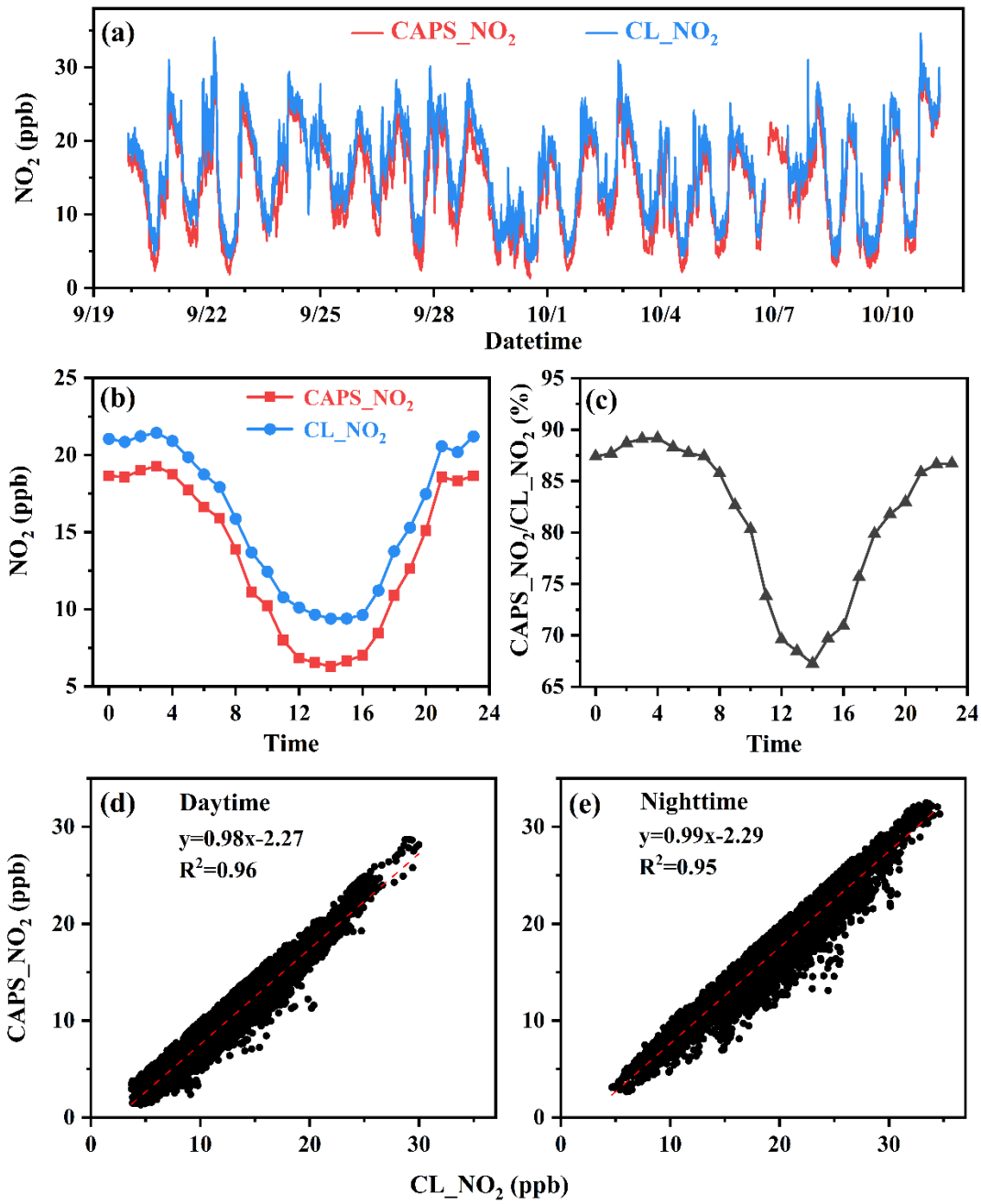

Figure S1 Time series (a) and diurnal variations (b) of CAPS_NO_2 and CL_NO_2, the diurnal variations of the fraction of CAPS_NO_2 in CL_NO_2 (c), and scatter plots with linear fits of CAPS_NO_2 versus CL_NO_2 during daytime (d) and nighttime (e).

Additionally, we sincerely appreciate the recommended reference, which provided valuable guidance for the NO_2 correction in this study. We added the relevant information and cited the suggested reference in the revised manuscript (Lines 120–122):

"The chemiluminescence (CL) technique could overestimate NO_2 concentrations due to interference from NOy (Villena et al., 2012; Wu et al., 2022a). Details of NO_2 correction were provided in Text S1 of the Supporting Information."

3. L123-124, delete the Wolfe et al before the bracket. It is the same for other similar references, such as Yan et al. (Yan et al., 2015), Zhang et al. (Zhang et al., 2019b), etc.

Response: Thanks for your valuable comments. Revision was made as the referee suggested. Deleted the Wolfe et al., Yan et al., and Zhang et al. before the bracket. Lines 130-131 and lines 318-321 in the revised manuscript:

"For more details on this part of the model, refer to (Wolfe et al., 2016)."

"For example, (Yan et al., 2015) and (Zhang et al., 2019b) reported that during haze pollution events in Beijing in the mid-2010s, the average $PM_{2.5}$ concentration could reach approximately 130 μg m^{-3}, with levels during severe haze episodes approaching 311 μg m^{-3}."

4. Figure 1 caption, it is better to define the meaning of DHP, PEP, and CLP. The meaning of the color bar in the 2nd subfigure should also be clarified.

Response: Thanks for your valuable comments. Revision was made as the referee suggested. In the caption of Figure 1, the meanings of DHP, PEP, and CLP are clearly defined, and the meaning of the color bar the 2nd subfigure is also specified. Additionally, "WD (°)" is also labeled in the 2nd subfigure. Lines 151-157 in the revised manuscript:

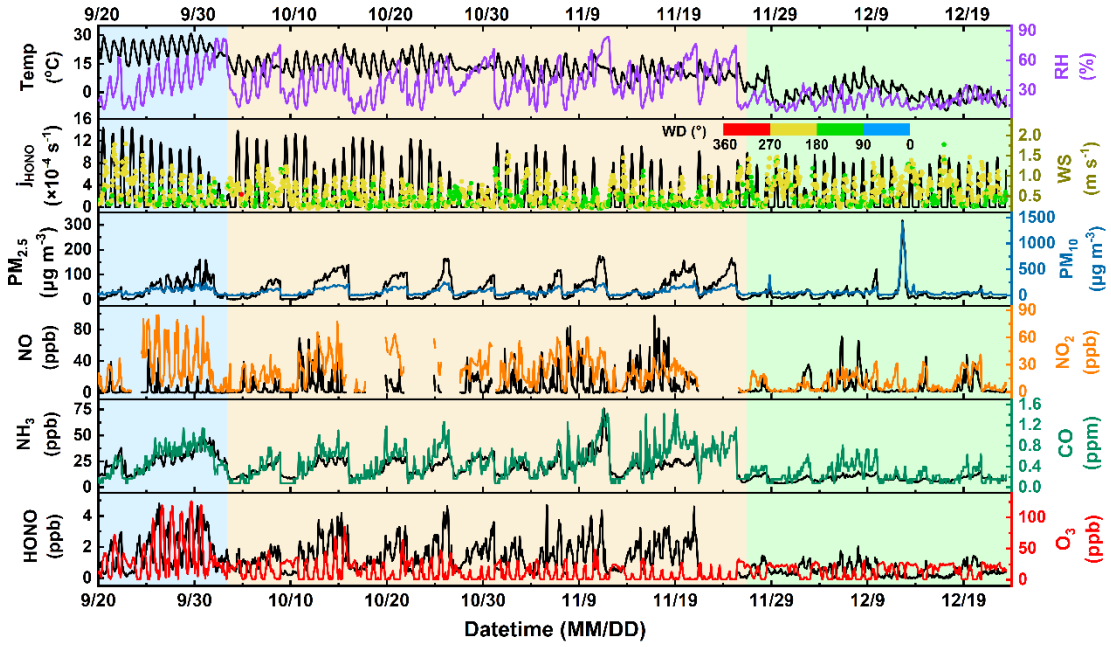

Figure 1: Hourly time series of meteorological parameters (Temp, RH, WS, j_{HONO}) and chemical species (HONO, O_3, NO, NO_2, NH_3, CO, $PM_{2.5}$, PM_{10}) concentrations from 20 September to 23 December 2022. The blue, yellow and green shades represent DHP, PEP and CLP, respectively. (DHP: Double-High Pollution Period, characterized by double-high levels of both O_3 and $PM_{2.5}$; PEP: $PM_{2.5}$ Episodic-cycle Pollution Period,

characterized by periodic cycle of $PM_{2.5}$ pollution; CLP: Clean Low Pollution Period, characterized by relatively low pollutant concentrations.) The color bar in the second subfigure represents wind direction (WD) in degrees.

5. L163-169, can you shortly explain the reasons why the pollutants concentrations are so low?

Response: Thanks for your valuable comments. During the CLP period (November 26 to December 23), pollutants concentrations were significantly lower, mainly due to a substantial reduction in anthropogenic activities. In urban Beijing, anthropogenic emissions are dominated by vehicle emissions. During the CLP period, the number of vehicles on the traffic arteries near the observation site decreased markedly, and traffic reports also showed a significant decline in the Traffic Performance Index (TPI), which indicates that the reduction in anthropogenic activities was the primary reason for the decrease in pollutants concentrations. The reasons for the reduced pollutants concentrations during the CLP period were also explained in detail in lines 258–264 of the manuscript.

6. The value used in Table 2 should be listed.

Response: Thanks for your valuable comments. The value used in Table 2 was listed as the referee suggested. Table 2 in the revised manuscript:

Source/ Loss	RACM Mechanisms	Parametrization
S_{emis}	Direct emission	$EF_{emis}=0.0051$
S_{NO+OH}	$NO + OH \rightarrow HONO$	k_{OH+NO}
$S_{NO_2\_g}$	$2NO_2 + H_2O \xrightarrow{\text{ground surface}} HONO + HNO_3$	$k_{het\text{-}g}=\frac{1}{8}\times v_{NO_2}\times\frac{1}{MLH}\times\gamma_g$
$S_{NO_2\_a}$	$2NO_2 + H_2O \xrightarrow{\text{aerosol surface}} HONO + HNO_3$	$k_{het\text{-}a}=\frac{1}{8}\times v_{NO_2}\times SA\times\gamma_a$
$S_{NO_2\_g,\,hv}$	$2NO_2 + H_2O + hv \xrightarrow{\text{ground surface}} HONO + HNO_3$	$k_{het\text{-}g,hv}=\frac{1}{4}\times v_{NO_2}\times\frac{1}{MLH}\times\gamma_{g,hv}\times\frac{j_{NO2}}{0.005s^{-1}}$
$S_{NO_2\_a,\,hv}$	$2NO_2 + H_2O + hv \xrightarrow{\text{aerosol surface}} HONO + HNO_3$	$k_{het\text{-}a,hv}=\frac{1}{4}\times v_{NO_2}\times SA\times\gamma_{a,hv}\times\frac{j_{NO2}}{0.005s^{-1}}$
$S_{pNO_3,\,hv}$	$pNO_3 + hv \rightarrow 0.67HONO + 0.33NO_x$	$k_{pNO_3,\,hv}=EF\times j_{HNO_3}$
L_{photo}	$HONO + hv \rightarrow OH + NO$	j_{HONO}
$L_{HONO+OH}$	$HONO + OH \rightarrow NO_2 + H_2O$	$k_{OH+HONO}$
L_{dep}	HONO deposition	$k=\frac{v_{HONO}}{BLH}$

As shown in Text S5 of the Supporting Information, the values of γ_g and $\gamma_{g,hv}$ were set to 2.94×10^{-6}, while the values of γ_a and $\gamma_{a,hv}$ were set to 3.12×10^{-5}. MLH was taken as 50 m in this observation to assess the ground-level sources of HONO (Lee et al., 2016; Xue et al., 2020; Xue et al., 2022). The enhancement factor (EF) was set to 30, a value commonly used in field observations conducted in autumn in Beijing (Zhang et al., 2022a; Xuan et al., 2024). The average dry deposition velocity of HONO (v_{HONO}) was taken as 2 cm s^{-1} (Harrison et al., 1996). k_{NO+OH}, $k_{OH+HONO}$, and j_{HNO3} were calculated in the RACM mechanisms. BLH represents boundary layer height, with units in meters (m).

7. L382-385, did you find any relationships between HONO concentrations and solar radiation? If you have, please show the data. Please refer to the publication: Explainable Machine Learning Reveals the Unknown Sources of Atmospheric HONO during COVID-19, ACS EST Air 2024, 1, 1252−1261.

Response: Thank you for your valuable comment and for recommending the reference. We analyzed the relationships between $HONO_{unknown}$, $P_{unknown}$, and solar radiation. Hourly solar radiation data were derived from the ERA5 reanalysis dataset (ECMWF). As shown in the revised Figure R1 (see below), $HONO_{unknown}$ exhibited a weak positive correlation with solar radiation ($R^2 = 0.23$), while $P_{unknown}$ showed a moderate positive correlation ($R^2 = 0.36$). These results indicated that both $HONO_{unknown}$ and $P_{unknown}$ were influenced by solar radiation. However, the degree of correlation differs. $P_{unknown}$ represented the production rate of HONO and was directly driven by photochemical processes during daytime, which were enhanced with increasing solar radiation. In contrast, $HONO_{unknown}$ concentrations were determined by a balance between production and removal processes (e.g., photolysis reaction, heterogeneous reaction and homogeneous reaction), which weakened its direct correlation with solar radiation. Therefore, the relatively stronger correlation observed for $P_{unknown}$ supported the hypothesis that unknown HONO sources were photochemically driven during daytime, while the weaker correlation of $HONO_{unknown}$ was consistent with its influence by multiple processes.

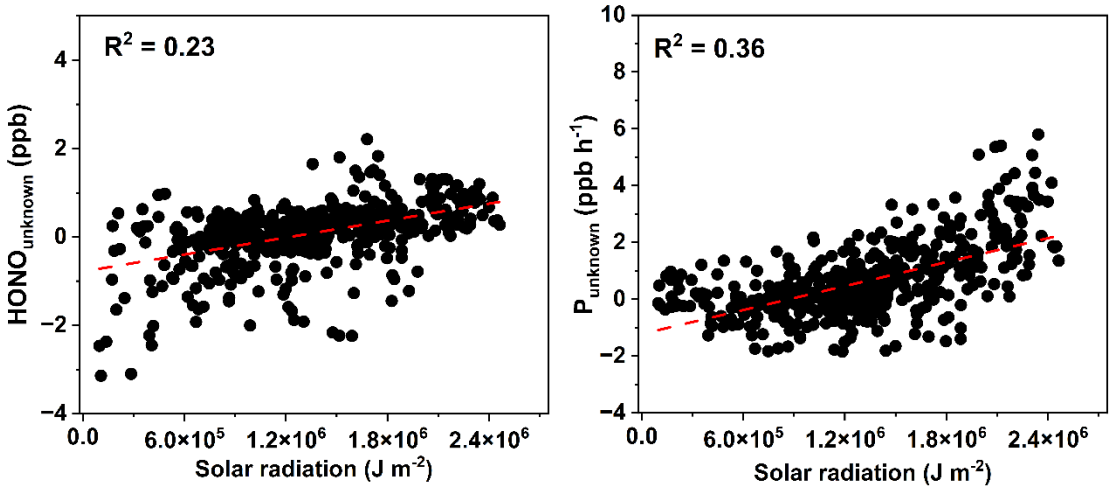

Figure R1. Correlations between $HONO_{unknown}$ and $P_{unknown}$ with solar radiation. The red dashed lines represent linear regression fits.

In addition, we carefully considered your advice and cited the recommended reference (Explainable Machine Learning Reveals the Unknown Sources of Atmospheric HONO during COVID-19, ACS EST Air, 2024, 1, 1252–1261) in the revised manuscript. Lines 411-413 in the revised manuscript:

"First, pathways related to solar radiation and OH radicals should be considered in future studies on daytime HONO sources, as also suggested by recent findings using explainable machine learning approaches (Gao et al., 2024)."

8. The implications of the research should be clarified. Such as in L419-433, the results may indicate that control vehicle emissions could be an effective measures to reduce air pollution, while more measures should be integrated during the haze periods.

Response: Thanks for your valuable comments. The implications of the research were clarified as the referee suggested. Lines 467-471 in the revised manuscript:

"These results had important policy implications for air pollution control. The study indicated that controlling vehicle emissions might be an effective measure to reduce HONO concentrations and improve air quality. However, during haze pollution periods, it is necessary to complement vehicle emission control with integrated multi-source measures, such as reducing NO_2 and NH_3 emissions, to limit the secondary formation of HONO and thereby more effectively reduce air pollution."

References

Gao, Z., Wang, Y., Gligorovski, S., Xue, C., Deng, L., Li, R., Duan, Y., Yin, S., Zhang, L., Zhang, Q., and Wu, D.: Explainable Machine Learning Reveals the Unknown Sources of Atmospheric HONO during COVID-19, ACS ES&T Air, 1, 1252-1261, 10.1021/acsestair.4c00087, 2024.

Harrison, R. M., Peak, J. D., and Collins, G. M.: Tropospheric cycle of nitrous acid, J. Geophys. Res. Atmos., 101, 14429-14439, 10.1029/96jd00341, 1996.

Kebabian, P. L., Wood, E. C., Herndon, S. C., and Freedman, A.: A practical alternative to chemiluminescence-based detection of nitrogen dioxide Cavity attenuated phase shift spectroscopy, Environ. Sci. Technol. , 42, 6040–6045, 2008.

Lee, J. D., Whalley, L. K., Heard, D. E., Stone, D., Dunmore, R. E., Hamilton, J. F., Young, D. E., Allan, J. D., Laufs, S., and Kleffmann, J.: Detailed budget analysis of HONO in central London reveals a missing daytime source, Atmos. Chem. Phys., 16, 2747-2764, 10.5194/acp-16-2747-2016, 2016.

Villena, G., Bejan, I., Kurtenbach, R., Wiesen, P., and Kleffmann, J.: Interferences of commercial NO2 instruments in the urban atmosphere and in a smog chamber, Atmos. Meas. Tech., 5, 149-159, 10.5194/amt-5-149-2012, 2012.

Wu, D., Zhang, J., Wang, M., An, J., Wang, R., Haider, H., Xu‐Ri, Huang, Y., Zhang, Q., Zhou, F., Tian, H., Zhang, X., Deng, L., Pan, Y., Chen, X., Yu, Y., Hu, C., Wang, R., Song, Y., Gao, Z., Wang, Y., Hou, L., and Liu, M.: Global and Regional Patterns of Soil Nitrous Acid Emissions and Their Acceleration of Rural Photochemical Reactions, J. Geophys. Res. Atmos., 127, 10.1029/2021jd036379, 2022a.

Xuan, H., Liu, J., Zhao, Y., Cao, Q., Chen, T., Wang, Y., Liu, Z., Sun, X., Li, H., Zhang, P., Chu, B., Ma, Q., and He, H.: Relative humidity driven nocturnal HONO formation mechanism in autumn haze events of Beijing, npj Clim. Atmos. Sci., 7, 10.1038/s41612-024-00745-8, 2024.

Xue, C., Ye, C., Kleffmann, J., Zhang, W., He, X., Liu, P., Zhang, C., Zhao, X., Liu, C., Ma, Z., Liu, J., Wang, J., Lu, K., Catoire, V., Mellouki, A., and Mu, Y.: Atmospheric measurements at Mt. Tai – Part II: HONO budget and radical (RO_x + NO_3) chemistry in the lower boundary layer, Atmos. Chem. Phys., 22, 1035-1057, 10.5194/acp-22-1035-2022, 2022.

Xue, C., Zhang, C., Ye, C., Liu, P., Catoire, V., Krysztofiak, G., Chen, H., Ren, Y., Zhao, X., Wang, J., Zhang, F., Zhang, C., Zhang, J., An, J., Wang, T., Chen, J., Kleffmann, J., Mellouki, A., and Mu, Y.: HONO Budget and Its Role in Nitrate Formation in the Rural North China Plain, Environ. Sci. Technol., 54, 11048-11057, 10.1021/acs.est.0c01832, 2020.

Zhang, J., Lian, C., Wang, W., Ge, M., Guo, Y., Ran, H., Zhang, Y., Zheng, F., Fan, X., Yan, C., Daellenbach, K. R., Liu, Y., Kulmala, M., and An, J.: Amplified role of potential HONO sources in O3 formation in North China Plain during autumn haze aggravating processes, Atmos. Chem. Phys., 22, 3275-3302, https://doi.org/10.5194/acp-22-3275-2022, 2022a.

Zhang, X., Tong, S., Jia, C., Zhang, W., Li, J., Wang, W., Sun, Y., Wang, X., Wang, L., Ji, D., Wang, L., Zhao, P., Tang, G., Xin, J., Li, A., and Ge, M.: The Levels and Sources of Nitrous Acid (HONO) in Winter of Beijing and Sanmenxia, J. Geophys. Res. Atmos., 127, 10.1029/2021jd036278, 2022c.